Structural modifications in the swelling of inhomogeneous microgels by light and neutron scattering

A. Fernández-Barbero,[1,*] A. Fernández-Nieves,[1,2] I. Grillo,[3] and E. López-Cabarcos[4]
[1]*Complex Fluid Physics Group, Department of Applied Physics, University of Almería, Cañada de San Urbano s/n, E-04120 Almería, Spain*
[2]*Department of Physics and DEAS, Harvard University, Cambridge, Massachusetts 02138*
[3]*Institut Laue-Langevin, F-38042 Grenoble, France*
[4]*Department of Pharmaceutical Chemical-Physics, University Complutense of Madrid, 28040 Madrid, Spain*
(Received 9 April 2002; published 11 November 2002)

Small-angle neutron scattering and dynamic light scattering have been used to study the thermodynamics of swelling and the associated structure modifications of highly cross-linked temperature-sensitive poly (*N*-isopropylacrylamide) [poly(NIPAM)] microgels in D_2O. A particle core-shell model is proposed, with the core containing most of the cross-linker molecules. The Flory-Rehner theory, with the inclusion of a concentration dependent Flory solvency parameter, successfully describes the experimental swelling, despite the inhomogeneous character of the particles. Interestingly, the shell evolution with temperature controls the whole particle swelling, exerting an external pressure over the core, which in turn influences its size during the swelling process. Scaling laws for the correlation lengths were found with respect to temperature and polymer concentration. Finally, it has been encountered that for the collapsed microgel states, the particle surface seems to have a fractal character.

DOI: 10.1103/PhysRevE.66.051803 PACS number(s): 61.25.Hq, 64.70.Nd, 83.10.Tv, 47.53.+n

I. INTRODUCTION

Synthetic polymer gels are known to exist in two phases, swollen and collapsed. The transition between the phases may occur either continuously or discontinuously, and provides a mean of studying the interactions between macromolecules. Many gels will undergo reversible volume changes in response to changes in external stimuli such as temperature, *p*H or light irradiation [1,2]. These transitions result from the competition between repulsive intermolecular forces and attractive forces due to the elastic behavior arising from the presence of cross links and hydrogen bonds.

Properties of swollen macrogels have been extensively studied by mechanical and thermodynamic experiments [3]. These include measurements of the shear and bulk moduli [4,5], diffusion constants of the network [6], specific heat [7], critical properties of gels in mixed solvents [8], and studies of spinodal decomposition processes [9], as well as of the effect of uniaxial and hydrostatic pressures on the transition [10]. It is well known that the volume fraction of networks at swelling equilibrium is fairly well predicted by the thermodynamic Flory-Rehner theory. However, the role of the structural changes that occur in such polymer networks is far from understood, mainly due to the spatial inhomogeneities introduced by the cross links. Scattering methods such as light scattering, small-angle x-ray and neutron scattering are usual techniques for studying these aspects of the volume phase transition [11].

Microgels form an interesting subset of polymer gels since they have properties in common with macrogels [12,13], as well as features typical of colloidal systems [14]. Like macroscopic gels, microgel particles also swell showing volume phase transitions. However, discontinuous phase changes have never been observed in microgel systems. Changes in the network structure during swelling drastically modify the hydrodynamics of the colloidal particles [15]. These changes control the topological mesoscopic structures and kinetics of growth in the event of colloidal aggregation [16,17], as well as the particle behavior under the presence of external electrical fields [18]. Furthermore, the modification of the short-range interactions between gel particles in the swelling has proven to lead to reversible aggregations [19].

Microgels have several advantages with respect to their extensive counterparts. For example, many potential applications of gel-like systems need very fast responses to external stimuli. Reducing the gel size to mesoscopic dimensions increases the time response by several orders of magnitude. Moreover, these systems have attracted a great interest when conceived as switchable or intelligent materials. The switch characteristic times can be reduced from several seconds for macrogels to a few milliseconds for mesoscopic gels [20].

Thermosensible microgels are monodisperse colloidal dispersions based on cross-linked polymers with low critical solution temperature. Most of them are based on poly (*N*-isopropylacrylamide) [poly(NIPAM)] or related copolymers. For these systems, all the properties are sensitive functions of temperature over the range 15–50 °C. At room temperature, these gels have a low refractive index difference with water due to the high water content. By contrast, at elevated temperatures, the particle volume is around an order of magnitude smaller, and thus, the refractive index difference with water is greatly increased.

Typical microgel preparations involve polymerization of NIPAM monomers whose chains are cross linked by *N*,*N*′-methylene bisacrylamide (BA) molecules. Wu *et al.* [21] studied the polymerization of NIPAM and BA during

*Email address: AFERNAND@UAL.ES

the microgel synthesis. The cross-linker molecules were found to be consumed quicker than the NIPAM molecules, indicating that the particles are unlikely to have a uniform composition. They also speculated that at least part of the cross-linker molecules could be located at the solvent/particle interface as a consequence of the larger hydrophobicity of poly(BA) as compared with poly(NIPAM).

In this paper, we take advantage of the different monomer conversion rates and employ a poly(NIPAM) microgel, highly cross linked with BA, for studying the structure of the resultant polymer network as it swells by small-angle neutron scattering (SANS). We also aim to elucidate the relationship between the microscopic structure modifications and the thermodynamics of swelling, which will be monitored by dynamic light scattering.

As a result of the particle inhomogeneous character, the SANS experiments showed two clearly distinguished zones corresponding to a core region of high monomer density and an outer shell, mainly formed by NIPAM chains. Interestingly, the microgel swelling is determined by the shell expansion that also tends to compress the particle core. The correlation lengths corresponding to the core and the shell have been obtained as a function of temperature and polymer concentration. The results show power law behavior, as encountered for macroscopic gels. However, differences in the scaling exponents are apparent. Furthermore, the particle surface in the collapsed phase shows a structured fractal surface, indicating that part some of the cross-linker chains could be located at the particle/liquid interface as predicted by Wu *et al.* [21].

From a thermodynamic point of view, we have employed the classical Flory-Rehner theory describing the swelling of thermosensitive homogeneous gels, despite the fact that the considered microgels present a clear core-shell structure. However, the fact that swelling is mainly controlled by the shell, allows this theory to describe fairly well the experimental continuous phase transition. In particular, we have used a fitting procedure that yields reasonable values for the parameters involved in the thermodynamic description of the swelling.

The outline of this paper is as follows. Section II is a theoretical background including a brief summary about the thermodynamics of thermosensible microgels and scattering functions for gels. Section III describes the experimental system and techniques. Section IV contains the experimental results and the discussion of these.

II. THEORETICAL BACKGROUND

A. Thermodynamics of polymer thermosensible microgels

Thermodynamic equilibrium for a gel is attained when the chemical potential of the solvent is equal inside and outside the gel, that is, when no net transfer of solvent takes place across the gel-solvent interface [22]. Thus, once equilibrium is reached, the net osmotic pressure within the gel must be zero.

The macroscopic state of a homogeneous neutral gel may be described through the total osmotic pressure inside the gel, which consists of two terms: mixing and elastic contributions. Within the classic Flory-Rehner theory of polymer gels, the net osmotic pressure is given by

$$\Pi = \frac{k_B T}{a^3}\left\{ -\phi - \ln(1-\phi) - \chi\phi^2 + \frac{\phi_0}{N_{\mathrm{gel}}}\left[\frac{1}{2}\left(\frac{\phi}{\phi_0}\right) - \left(\frac{\phi}{\phi_0}\right)^{1/3}\right]\right\}, \tag{1}$$

where k_B is the Boltzmann constant, χ is the Flory solvency parameter, ϕ_0 is the polymer volume fraction at a reference state, a is the monomer segment length, and N_{gel} is the average degree of polymerization of the polymer chain between cross links. For systems undergoing isotropic swelling, the following relationship between the diameter of a spherical microgel, D, and the average polymer volume fraction ϕ holds:

$$\frac{\phi}{\phi_0} = \frac{V_0}{V} = \left[\frac{D_0}{D}\right]^3, \tag{2}$$

with V_0 and D_0 being the particle volume and particle size at the reference state.

A proper thermodynamic description for the volume changes of thermosensible microgels follows from the assumption of isobar conditions, described under the constraint $\Pi = 0$. In the T-ϕ phase diagram, the isobar line is given by [23]

$$T_{\pi=0} = \frac{A\phi^2\Theta}{\frac{\phi_0}{N_{\mathrm{gel}}}\left[\frac{1}{2}\left(\frac{\phi}{\phi_0}\right) - \left(\frac{\phi}{\phi_0}\right)^{1/3}\right] - \phi - \ln(1-\phi) + \left(A - \frac{1}{2}\right)\phi^2}, \tag{3}$$

where $A = (2\Delta S + k_B)/2k_B$ and $\Theta = 2\Delta H/(2\Delta s + k_B)$. ΔS and ΔH are the changes in entropy and enthalpy of the process, respectively.

Equation (3) predicts first-order phase transitions between swollen and deswollen phases. The mechanism driving the transition is entirely incorporated into χ. The meaning of χ is similar to that of the parameter expressing the contact energy change appearing in the Bragg-Williams theory for order-disorder transitions in alloys [24]. Writing the change in the free energy per solvent molecule induced when a solvent-solvent contact is changed into a solvent-polymer contact as ΔF, the parameter χ is defined as

$$\chi = \frac{\Delta F}{k_B T} = \frac{\Delta H - T\Delta S}{T k_B} = \frac{1}{2} - A\left(1 - \frac{\Theta}{T}\right). \tag{4}$$

Usually, molecular interactions contribute to both ΔS and ΔH, the sign of both quantities being the same. Polymer-solvent systems possessing an upper-critical-solution temperature (UCST) are characterized by positive values of ΔS and ΔH, while the others with a the lower-critical-solution temperature (LCST) are characterized by negative values of

them. For $T=\Theta$, the Flory χ parameter equals $\frac{1}{2}$, and the system is in the so-called Θ temperature, where binary interactions are negligible and only excluded volume effects are important. In this work, both Θ and A will be used as fitting parameters allowing ΔS and ΔH to be determined.

B. Scattering functions for gels

SANS is a widely used technique for investigating the structure of polymer networks. SANS experiments consist of the measurement of the scattered intensity $I(q)$ as a function of the scattering vector q, which is related to the neutron wavelength λ and the scattering angle θ by $Q=(4\pi/\lambda)\sin(\theta/2)$. The elastic scattered intensity $I(Q)$ in absolute intensity scale is given by $I(Q)=I_{\mathrm{obs}}(Q)-I_{\mathrm{inc}}(Q)$, where $I_{\mathrm{obs}}(Q)$ and $I_{\mathrm{inc}}(Q)$ are the observed scattering intensity and the incoherent scattered intensity, respectively [25].

In the case of polymer solutions in the semidilute regime, the elastic scattered intensity is usually characterized by one single length scale, namely, the correlation length, defined as the characteristic size of the polymer concentration fluctuations. It enters the correlation function for the polymer concentration in the limit $r \geqslant \xi$ as [26]

$$\langle \phi(0)\phi(r)\rangle \sim \frac{1}{r} e^{(-r/\xi)} \quad \text{for } r \geqslant \xi, \tag{5}$$

Equation (5) establishes that polymer concentration fluctuations can be considered as essentially uncorrelated on length scales larger than ξ. In a good solvent, this means that the correlation length is roughly equal to the average distance between interchain contact points. In poor solvents, this is no longer valid [27].

When a contrast is established between all the chains and the solvent, the neutron scattering intensity is proportional to the Fourier transform of Eq. (5) in the limit $Q\xi<1$. Thus, $I(Q)$ is expected to be given by an Ornstein-Zernicke-type function [25]:

$$I(Q)=\frac{I(0)}{(1+\xi^2Q^2)}, \quad \text{for } \xi Q<1, \tag{6}$$

where ξ is the correlation length that indicates the mesh size or blob composing polymer chains. This characteristic length is expected to scale with polymer volume fraction as [28]

$$\xi \sim \phi^{\nu_\phi}, \tag{7}$$

where the exponent $\nu_\phi=-\nu_F/(3\nu_F-1)$, is related to the Flory's excluded volume exponent ν_F, which is equal to 3/5 for good solvents (self-avoiding walk) and to $\frac{1}{2}$ for Θ solvents (random walk). Thus, ν_ϕ takes the values $-3/4$ for good solvents and -1 for Θ solvents. This parameter is an indirect measurement of the interactions between chains, through the modification that those interactions produce on the excluded volume effect.

The Ornstein-Zernicke function (6) obtained under the semidilute assumption has proven to be also valid to describe the neutron scattering spectrum from a gel [11]. When cross links are introduced to these polymer solutions, the concentration fluctuations are perturbed. The exact solution for the scattering function from gels has not been developed yet because of the complexity and variety of cross-link formation. However, several scattering functions have been proposed. Hecht, Duplessix, and Geissler [29] separated the scattered intensity function into two terms arising from solutionlike and solidlike concentration fluctuations. The solutionlike concentration fluctuations was assumed to be the same to the corresponding polymer solution. On the other hand, Horkay and co-workers [30,31] assumed that the solidlike concentration fluctuations had an exponential form and proposed a scattering function for chemically cross-linked gels, given by

$$I(Q)=I_G(0)e^{-\Lambda Q}+\frac{I_L(0)}{(1+\xi^2Q^2)}, \tag{8}$$

where Λ is the mean size of the solidlike (static) nonuniformity. $I_G(0)$ and $I_L(0)$ are constants that depend on the relative contribution of the two terms.

By contrast, for $r<\xi$, a part of the chain behaves essentially as if it was not interacting with other chains. The average conformation is then ruled by the excluded volume statistics alone. In this spatial range, the correlation function of the concentration fluctuations therefore equates to that of a single chain:

$$\langle \phi(0)\phi(r)\rangle \sim r^{-4/3} \quad \text{for } r<\xi. \tag{9}$$

The scattered intensity is related to the Fourier transform of Eq. (9). Thus, for $Q\xi>1$ and $Qa<1$, with a being the statistical unit length, $I(q)$ is given by

$$I(Q)\sim Q^{-1/\nu_F}. \tag{10}$$

For colloidal gels, the particle form factor cannot be neglected [32]. For particles with $R_G \gg Q^{-1}$, only the Porod region of $P(Q)$ should contribute significantly to the scattering intensity. As a consequence, the scattering arises also from the particle surface and thus the data should be described by expressions of the type

$$I(Q)=\frac{A}{V}\frac{1}{Q^4}+\frac{I_L(0)}{(1+\xi^2Q^2)}, \tag{11}$$

where A is the interfacial area in the scattering volume V. The contribution from the crosslinks is omitted for the scattering description used in this paper since exponential profiles were never observed. For shrunk systems, the scattering should mainly arise from the interface between the collapsed polymer particle and the surrounding solvent. In the case of smooth interfaces, $I(Q)$ is described by Porod's law, $I(Q)\sim Q^{-4}$.

III. EXPERIMENT

A. Experimental system

Poly(NIPAM) microgel particles were prepared using surfactant-free, free radical polymerization in water. Water (Milli-Q quality) containing NIPAM (Kodak Eastmann) and

N, *N'*-methylenebisacrylamide (Aldrich) was adjusted to *p*H 9 with NaOH and was placed in a three-necked, round-bottomed flask equipped with a stirrer paddle, immersed in an oil bath at 343 K. Amonic persuphate (Aldrich) employed as initiator was dissolved in water at *p*H 11 and added to the flask. The polymerization was conducted under anaerobic conditions, having nitrogen gas entering at one neck and a water-cooled condenser at the other. The reaction was then left for 6 h, resulting in a milky white dispersion. The system was allowed to cool and then filtered through glass wool before being extensively dialysed against distilled water, changing the dialysate twice a week. Once the microgel was purified, it was further dried under vacuum. Samples were prepared by dissolving the dry polymer in D_2O. The cross-linking degree was 10 wt % [33].

B. Dynamic light scattering

Dynamic light scattering (DLS) experiments were conducted in order to examine the particle size upon a change of temperature. The time correlation function of the scattered intensity, $\langle I(0)I(\tau)\rangle$, was measured by laser light scattering spectroscopy. A Malvern 4700 system (UK) working with a 6328-Å-wavelength He-Ne laser was employed. The scattering angle was set to 40°. The mean hydrodynamic radius was obtained as a function of temperature, using cummulant analysis. Temperature was controlled with a precision of 0.1 K, using both a peltier cell located just into the index matching liquid that surrounds the sample cell and an external bath acting through the sample chamber. Particle concentration in D_2O was kept dilute (0.03 wt %) to diminish colloidal interactions as well as multiple scattering, which could mainly appear when particles are in the collapsed state.

C. SANS experiments

SANS experiments were performed using the *D*11 spectrometer at the ILL facility (Institut Laue-Langevin, Grenoble, France) [34]. A cold neutron flux having the average wavelength of 6 Å with a spread of 10% was used as the incident beam, by setting the mechanical selector at 21126 rpm. In order cover a large angular range, three instrumental settings were used: the 64×64 cm^2 gas filled detector, having a resolution of 1 cm^2, was placed 1.2 m apart from the sample for large angles, 5.5 m for middle angles, and 10.5 m for small angles. The resultant Q range was 0.005–0.303 Å^{-1}. The detector efficiency was corrected using H_2O as entirely incoherent scatterer standard. Data reduction was performed by correcting the direct scattered counts for dark scattering (using a Cd sheet located at the sample position), for cell scattering, and D_2O scattering, as well as for transmission. For data reduction, the usual programs at the ILL facility were employed. The contribution of the incoherent scattering due to hydrogen was also corrected by assuming the additivity of the incoherent scattering between NIPAM and D_2O. Microgel particle concentration in D_2O was 4 wt %. All samples were contained in 1-mm-path Hellma quartz cells, and prior to undertaken the measurements, cells were kept for 15 min in the instrument temperature-controlled chamber, allowing for temperature stabilization. Temperature was controlled with a precision of 0.1 K.

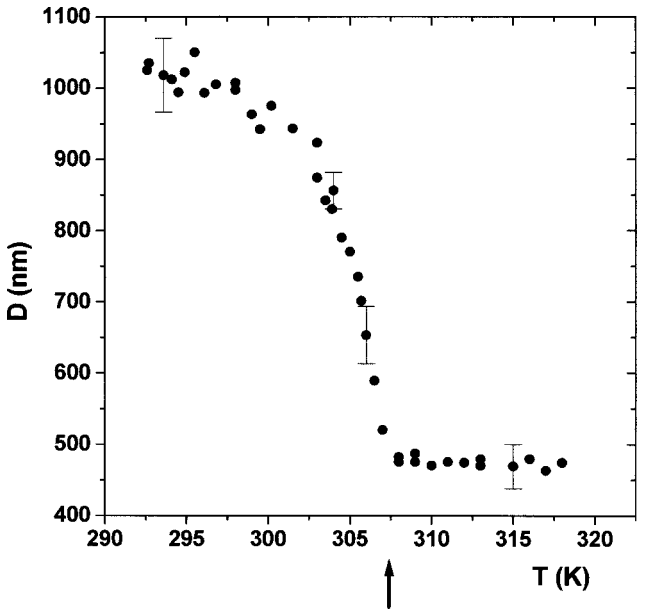

FIG. 1. Experimental mean hydrodynamic particle diameter versus temperature. The arrow indicates the transition temperature.

IV. RESULTS AND DISCUSSION

A. Thermodynamics of the volume phase transition

In this section we determine the temperature dependence of the microgel size and compare the results with the predictions of the Flory-Rehner phenomenological theory, employed for describing the swelling of thermosensitive macroscopic gels. The comparison allows us to test how well can this theory account for the volume transition of microgels.

Figure 1 shows the experimentally determined diameter (using DLS) of the microgel particles, *D*, as a function of temperature. As can be observed, *D* decreases gradually with temperature until a sharp but continuous volume transition from swollen to deswollen states takes place, reaching a final collapsed size at a transition temperature $T_c \cong 307$ K. This process was thermoreversible without any significant hysteresis. It is well documented in the literature [35] that poly(NIPAM) particles in H_2O show a maximum rate of deswelling at 305 K. In D_2O, however, the corresponding temperature shifts to 307 K, which agrees with our results and those reported by Shibayama, Tanaka, and Han for poly(NIPAM) macrogels [36]. This temperature may be taken to be the LCST for the poly(NIPAM)/D_2O system, as will be proven at the end of the section.

The microgel size variation is controlled by the Flory χ parameter, which is the central variable governing the thermodynamics of swelling. According to the definition, χ should be independent of composition for a given polymer-solvent pair. Experimentally, however, it has been encountered that χ increases nonlinearly with increasing concentration of polymer [37]:

$$\chi(T,\phi)=\chi_1(T)+\chi_2\phi+\chi_3\phi^2+\cdots. \qquad (12)$$

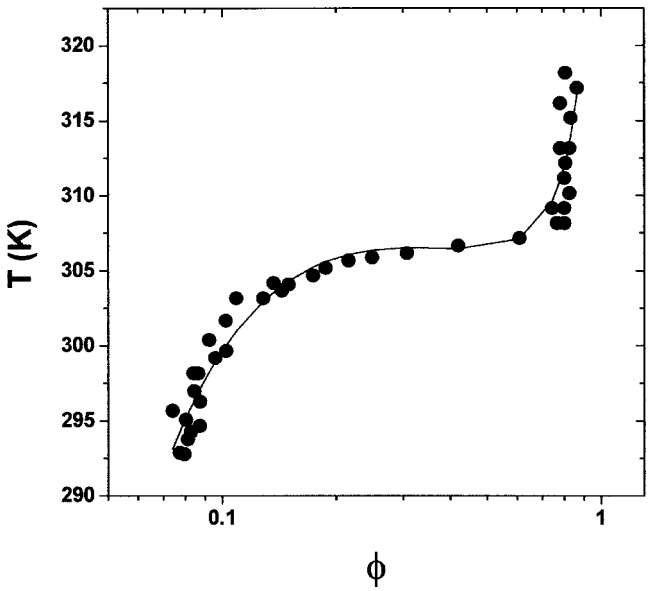

FIG. 2. Phase diagram of poly(NIPAM)/D_2O system. The solid line is the theoretical prediction including the first-order concentration dependence of χ. The values of the fitting parameters were $\phi_0=0.8$, $A=-7$, $\Theta=308$ K, $N_{gel}=7$, and $\chi_2=0.9$.

This fact is not included in the above theory. However, the cause of this discrepancy continues being one of the basic problems in the theory of polymer solutions. In addition, the proper choice for the reference volume fraction ϕ_0 is not clear. In some cases, this constant has been set equal to one for the collapsed state, obtaining fairly good results, for example, when describing the swelling of ionized vinilpyridine microgels [13]. In other cases, the particle size in the collapse state seems to depend on the nature of the solvent [38], which means that ϕ_0 should not necessarily be 1. Recent nuclear-magnetic-resonance measurements lead to the same conclusion [39]. In the present paper, the assumption $\phi_0=1$ leaded to catastrophic results. For this reason, the reference volume fraction was modified in the fitting procedure (described below), since no direct measurements of this variable are available.

In order to model the experimental results, Eq. (1) was employed under the assumption $\Pi=0$, substituting the expression of $\chi(T,\phi)$ till second order. The assumption that χ_2 and χ_3 are not temperature dependent is used as a good approximation. The fit to the experimental T-ϕ curve is presented in Fig. 2. The values $\phi_0=0.6$, 0.7, 0.8, 0.9, where tested, considering (i) zero-order ($\chi_2=\chi_3=0$), (ii) first-order ($\chi_3=0$), and (iii) second-order approximations. The resultant fitting parameters for each case are summarized in Table I. Due to the great deal of variables involved in the fitting procedure, almost every solution could be valid under visual inspection of Fig. 2. However, by comparing the obtained parameters with the values obtained by independent techniques and the necessary boundings to ensure physically meaningful results, the best fit can be adequately established. There are three conditions that the solution must satisfy: (i) the values for A and Θ should lead to a reasonable behavior of $\chi_1(T)$. Indeed, χ_1 must be within the range 0–1. (ii) The Θ temperature and the transition temperature (307 K) should be close. This fact yields to the second-order approximation exclusion. (iii) The number of monomers between cross links should not be too far from the value obtained from neutron scattering measurements. As will be shown in the following section, the swelling of the microgel particle is controlled by the volume changes of the shell, whose characteristic blob length in the swollen state is 39 ± 3 Å (see Fig. 6a). This value yields $N_{gel}^{SANS}=(4.8\pm0.4)$, since the segment length of the NIPAM monomer is 8.12 Å [40,41]. Values far from this estimate should not be considered, ruling out some of the situations shown in Table I.

As a result, the only valid solution was obtained considering a first-order approximation for the Flory solvency parameter and a value for the collapsed polymer volume fraction $\phi_0=0.8$. The values for $\phi_0=0.9$ are close to those obtained for $\phi_0=0.8$, except the A parameter changing from -7 to -49. That difference is significant since the fitting error for parameter A is $\approx$30%. The solution for $\phi_0=0.9$ was rejected since it deals to acceptable χ values (within the range 0–1) only in the range 303–308 K, which implies that this solution cannot describe the T-ϕ phase diagram.

From the obtained values for all parameters at $\phi_0=0.8$, several conclusions can be extracted:

(i) Around 20% of the microgel particle in the collapsed state, corresponds to solvent molecules. This fact agrees with previous investigations in which the microgel particles are slightly swollen in the shrunken state [20,38,39].

(ii) The first-order approximation is necessary in order to describe the microgel particle swelling. A value of $\chi_2=0.9\pm0.1$ was used in the fit. Within the Flory theory of gels, the concentration dependence of χ is the driving characteristic for the transition in neutral gels. A particular strong concentration dependence of χ is essential for a discontinuous tran-

TABLE I. Fitting parameters used to model the experimental results [see Eq. (11) and Fig. 2].

	$\chi=\chi_1(T)$				$\chi=\chi_1(T)+\chi_2\phi$				$\chi=\chi_1(T)+\chi_2\phi+\chi_3\phi^2$			
ϕ_0	0.6	0.7	0.8	0.9	0.6	0.7	0.8	0.9	0.6	0.7	0.8	0.9
A	−20	−29	−44	−79	−3	−5.8	−7	−49	−6.4	−10	−18	−93
Θ	306.8	306	307	307	313	312	308	308	315	314	313	314
N_{gel}	85	51	30	14	419	188	7	6	177	93	8	8.7
χ_2					0.64	0.76	0.91	0.87	1.4	1.6	1.85	8.5
χ_3									−1.04	−1.07	−1.03	−7.5

sition to occur in neutral gels [42]. The theoretical critical value of χ_2 is 1/3 for a gel with infinitely long chains. In most situations, however, the critical value appears to be larger than this value. As a result, a discontinuous transition rarely occurs in neutral gels because it requires an unusually large concentration dependence of χ. The discontinuous transition may be observed for NIPAM macrogels with small cross-link density [3,43,8]. The value obtained by Hirotsu for discontinuous transitions in poly(NIPAM) macrogels was $\chi_2=0.6\pm0.1$. As can be observed for poly(NIPAM) microgel particles, even with a larger concentration dependence, discontinuous transitions are not observed. In order to understand the mechanism of the phase transition of gels on a molecular level, the microscopic interaction that makes χ depend on the concentration must be identified, but even for neutral gels, this is a very complicated problem. Calculations by Hocker, Shih, and Flory [44] on the basis of statistical thermodynamic theories are unapplicable to the complex case considered here.

(iii) The Θ temperature, 308.0 ± 0.3 K, and the transition temperature, 307.2 ± 0.1 K, are in good agreement as expected since this is one of the criteria used to refuse other solutions. The acceptance as valid of any other solution with the fitting temperature Θ close to the experimental transition temperature, but exhibiting a wider difference should imply that the microgel does not start to swell just when the liquid changes from a poor solvent to a Θ solvent.

(iv) The values of A and Θ allow determination of the entropy and enthalpy variation when a solvent-solvent contact is changed by a polymer-solvent one. The calculated values are $\Delta S=(-1.1\pm0.8)\times10^{-22}$ J/K and $\Delta H=(-3\pm1)\times10^{-20}$ J. The negative sign of ΔS and ΔH indicate the LCST nature of poly(NIPAM)/D_2O system. $|\Delta H|$ is larger than k_BT for this system, explaining the strong volume dependence that the microgel exhibits with temperature.

(v) As an overall result, the Flory-Rehner theory describing the swelling of neutral gels captures the essential physics, as can be deduced from the fact that all fitted parameters show reasonable values. In view of its simplicity, it is remarkable that this is indeed the case.

B. Structural aspects of the volume phase transition

Small-angle neutron scattering from poly(NIPAM) microgel particles was recorded at different temperatures: 293, 298, 302, 303, 305, 306, 308, and 314 K. The scattering profiles decreased monotonously with increasing wave vector for swollen and collapsed microgel states. Dynamic concentration fluctuations as well as permanent departures from uniformity due to cross links contribute to the scattering intensity. However, the difference in the neutron scattering length density between the sample and the surrounding medium [contrast term $(\Delta\delta)^2$] is one order of magnitude larger for the NIPAM molecules than for the BA molecules. Consequently, the exponential term coming from the solidlike concentration fluctuations is not observed. Log-log plots of some representative scattering curves are shown in Fig. 3. Three regions are distinguished in the scattering curves. At low angles, the scattered intensity increases with increasing temperature, reaching a near Porod profile, $\sim Q^{-4}$. Thus, this scattering region is mainly dominated by the scattering from the particles surfaces. At larger Q values, the scattering intensity shows two power laws in Q with a break point between both regions (Q_o). The presence of these two regions indicates that particles have a structural inhomogeneity. In particular, a core-shell structure where both domains show different structural density is compatible with this scenario, the core dimensions being related to the characteristic length coming from the break point Q_0. For even larger Q values, the scattering profile is related to the excluded volume Flory exponent.

The low-Q scattering region is characterized by a decreasing power law, $Q^{-\alpha}$. Figure 4 plots the exponent α as a function of the temperature. For swollen particles, the exponent value is typical of extended polymer branches [25]. As the particles deswell, the scattering exponent increases, reaching values that are slightly higher than 4. Similar results were also found by Kratz, Hellweg, and Eimer [45]. These values are not too far from the typical ones corresponding to three-dimensional objects with smooth surfaces. The resulting SANS profiles are then dominated by scattering from the interfaces between the colloidal particles and the surrounding solvent. However, these slight differences seem to indicate that the particles surfaces could have a fractal structure. In line with this possibility, Wong [46] found scattering exponents larger that 4 for known fractal surfaces. Thus, the Q^{-4} dependence in the Porod regime must be modified by an additional contribution, $I(Q)\sim Q^{-6+d_s}$, where d_s is the surface fractal dimension. For smooth surfaces, $d_s=2$, and the Porod law is fulfilled. In the inset of Fig. 4, the extracted surface fractal dimensions are presented. As can be observed, d_s decreases as temperature raises. Due to the high hydrophobicity of the poly(BA) molecules, two types of domains my be present on the gel surface [21]; one prominently poly(BA), which is not temperature sensitive, the other poly(NIPAM), which is. When such structure is heated, surface roughness should increase and the corresponding fractal dimension will decrease.

The scattering Q regions corresponding to the shell and core are well described by the Lorentzian curve of Eq. (6). From the slopes and intercepts of linear fits in the Ornstein-Zernike representation [$I^{-1}(Q)$ vs Q^2 plot], the characteristic correlation lengths for the core and shell, ξ_{core} and ξ_{shell} can be determined. As an illustration, Fig. 5 shows the *O-Z* plot corresponding to the swollen state. In this, the three scattering regions corresponding to the surface, shell, and core can be identified. Figure 6(a) plots the resultant shell and core correlation lengths as a function of the temperature. The first remarkable feature is related to the inhomogeneous character of the particle. At low temperature, the correlation lengths are quite different, being $\xi_{\text{core}}<\xi_{\text{shell}}$. This fact indicates that the nature of the inhomogeneity responsible for the core-shell structure may be related to the accumulation of cross linker into the core.

The shell correlation length is constant above the transition temperature, while it increases drastically from ~8 to ~40 Å as the temperature is decreased, following the whole particle size behavior as determined by dynamic light scat-

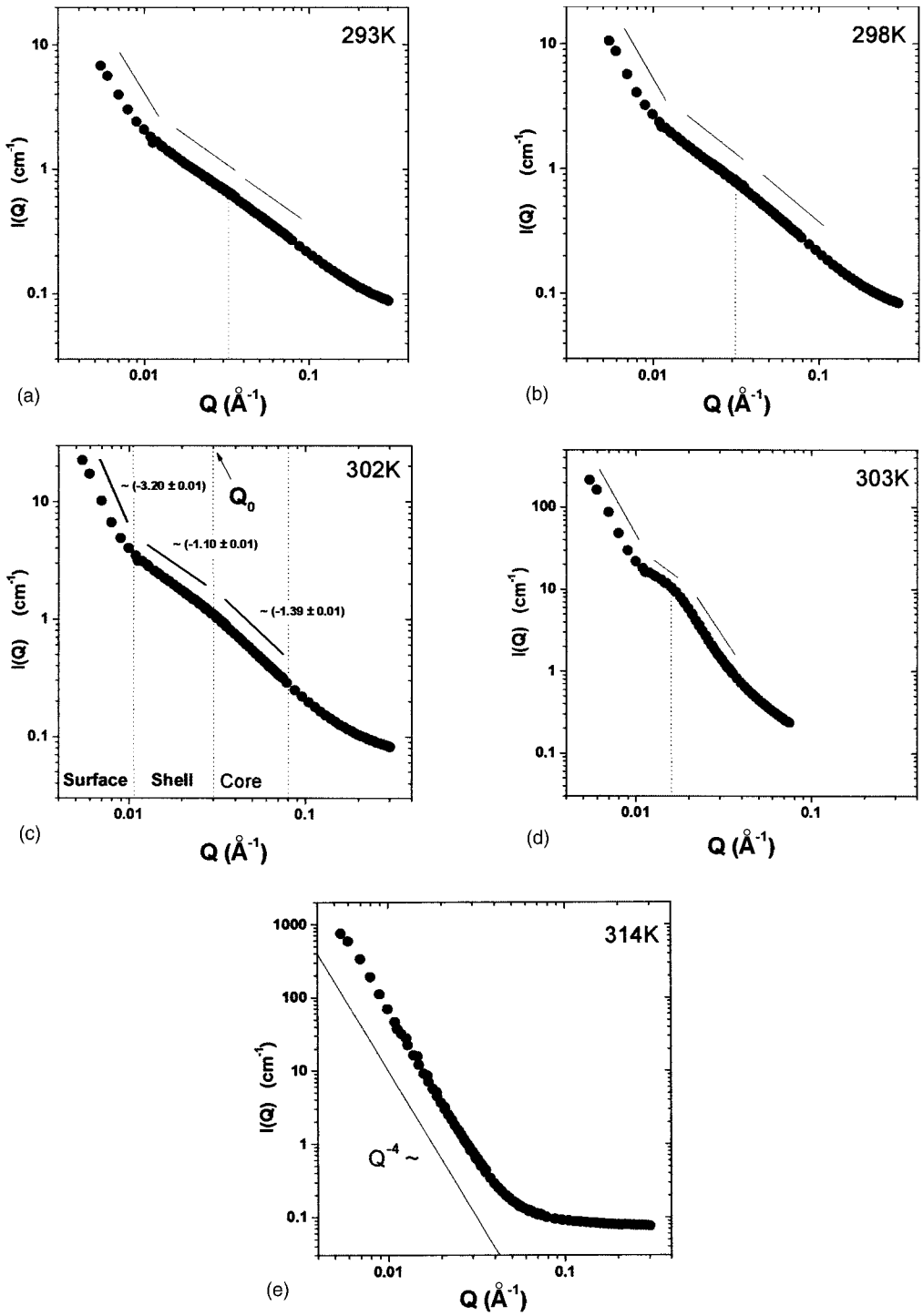

FIG. 3. Double logarithmic plot of SANS intensity functions at different temperatures. (c) illustrates the three scattering zones defined for data interpretation, which correspond to particle surface effects, particle shell, and core. (e) also plots the Porod function corresponding to smooth scattering surfaces.

tering (Fig. 1). It is worthy to mention that the characteristic distance between cross links, calculated from the polymerization degree in the Flory-Rehner theory is of the order of the value obtained, as already pointed out before (Sec. IV A).

Figure 6(a) also plots the correlation length of the core network, which also remains constant for temperatures corresponding to particle collapsed states. In this region, $\xi_{\mathrm{core}} \leqslant \xi_{\mathrm{shell}}$, in agreement with what could be expected because of the higher elastic shrinking component of the core due to the presence of a higher cross-linker concentration. The characteristic core blob size increases from ~8 to ~18 Å as temperature is diminished, as a consequence of the variation of the polymer solvency and following the shell size growth. However, the correlation length decreases again as the temperature is further reduced. This result agrees with the fact

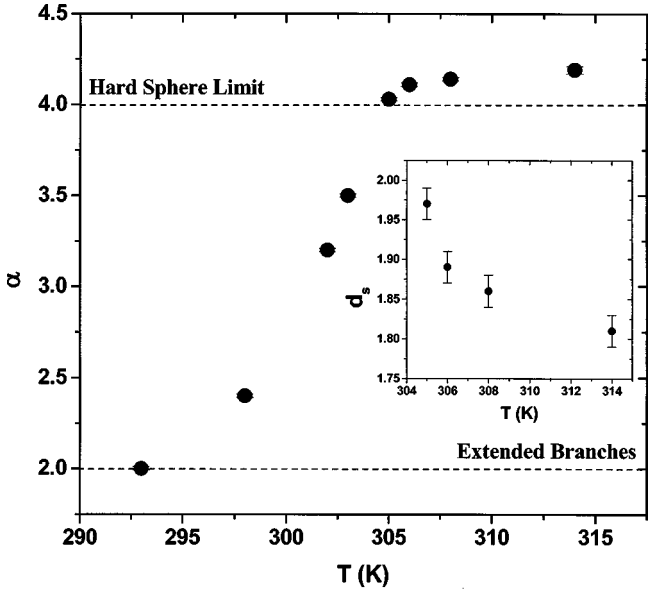

FIG. 4. Exponent α as a function of temperature during the swelling process. At low temperature (swollen state), the exponent corresponds to extended polymers branches. Beyond the transition temperature, the value slightly larger than 4 indicates deviation from smooth surfaces, being the particle surface characterized by a fractal structure. The surface fractal dimension is plotted in the inset.

that Q_0, which is related to the particle core size (Fig. 3), shifts towards larger values as the temperature is decreased, indicating that the core size also decreases, as plotted in Fig. 6(b). This is an interesting and somewhat unexpected result. However, it follows from the fact that the polymer solvency increases as the temperature is decreased, implying that the polymer in the shell expands. This originates in an increase in particle size, but also and simultaneously, in a reduction in core dimensions since the shell also tries to expand towards the inner particle region. Thus, the particle core shrinks at

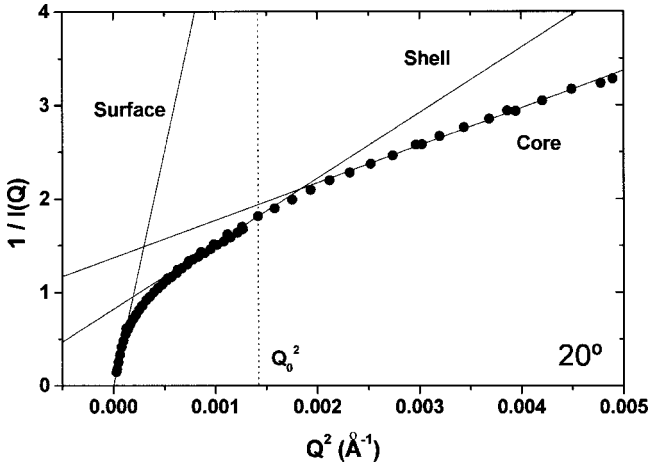

FIG. 5. Ornstein-Zernike representation of the scattering spectrum for the system at the swollen state. From the slope and intercept, the characteristic correlation blob length is determined for the particle shell and core.

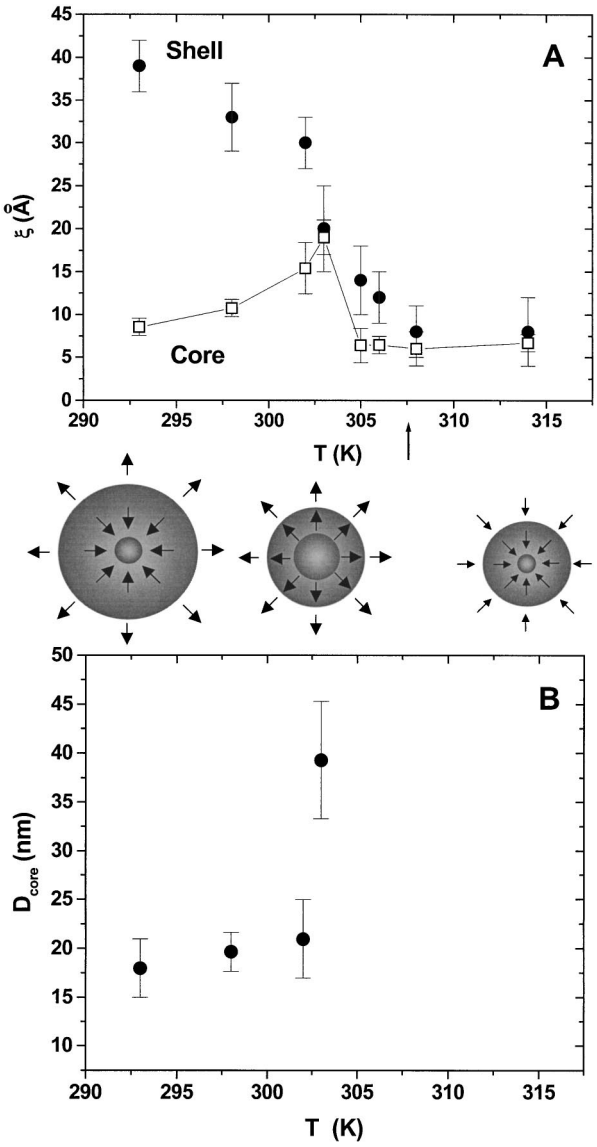

FIG. 6. (a) Temperature dependence of the characteristic correlation lengths for the particle core and shell. (b) Estimation of the core size from the Q_0 break point in Fig. 3. The sketch shows the core and shell behaviors during the phase transition.

low temperature as a consequence of the interaction with the shell. It is interesting to point out that the core blob length becomes constant at temperatures greater than 304 K; this is at ~3 K below the transition temperature for the polymer. For 304 K$<T<T_c$, the shell is still swollen and thus exerting pressure over the core. This fact is then responsible for the core transition temperature shift to lower values.

C. Scaling rules for microgels

The correlation length for the particle shell is plotted as a function of the volume fraction calculated from DLS measurements in Fig. 7. ξ_{shell} scales as a power law, with a scaling exponent $\nu_\phi = -0.79 \pm 0.06$. This is in good agreement with the theoretically predicted value for semidilute polymer

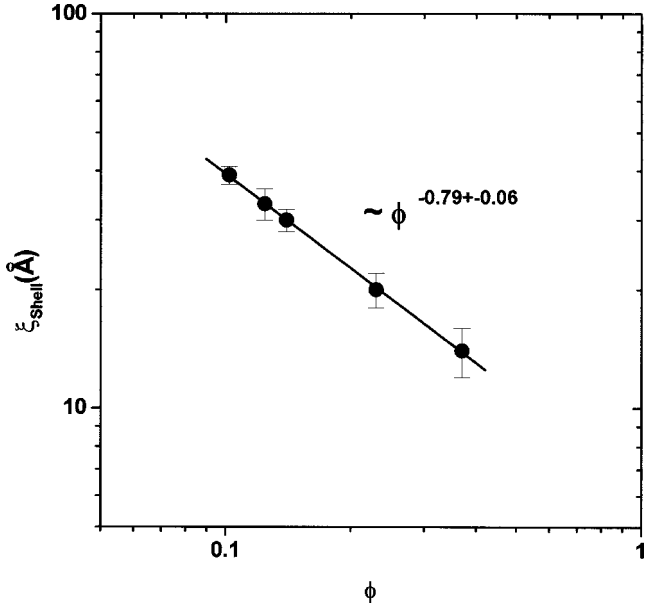

FIG. 7. Scaling of the shell correlation length with the polymer concentration.

solutions in a good solvent ($\nu_\phi^{\text{theory}} = -\frac{3}{4}$), corresponding to a excluded volume Flory parameter $\nu_F = 3/5$, typical of self-avoiding walks.

The experimental value for the poly(NIPAM) microgels agrees with that obtained for NIPAM homopolymer solutions for temperatures far below the transition temperature [36]. However, in that case a temperature-dependent ν_ϕ was encountered. For the poly(NIPAM) microgels, ν_ϕ seems to be temperature independent, as already found for macroscopic gels. Nevertheless, the measured value is quite far from those measured by Shibayama, Tanaka, and Han [36] (-1.1 to -1.2) for NIPAM homopolymer macrogels.

The ϕ dependence of the core correlation length was also studied. As expected, the results did not show a power law behavior mainly due to the shell pressure during the swelling process, which hinders the free swelling of the core.

Finally, we will explore the temperature dependence of the core correlation length and $I(0)$. In a first-order phase transition, both of them should diverge at the spinodal temperature T_s, following the relationships: $\xi \sim |T_s - T|^{-\nu}$ and $I(0) \sim |T_s - T|^{-\gamma}$. Figure 8 shows log-log plots of ξ and $I(0)$ as a function of the temperature increments for the poly(NIPAM) microgel. The spinodal temperature has been identified with the transition temperature. The exponents from the linear fits are $\nu = -0.63 \pm 0.04$ and $\gamma = -0.92 \pm 0.05$. Due to the restricted number of data points, the estimated exponents should only be taken as approximate. Nevertheless, both values are not far from those predicted for gel systems using the three-dimensional Ising model [47,48]. In addition, they agree with the experimental values measured

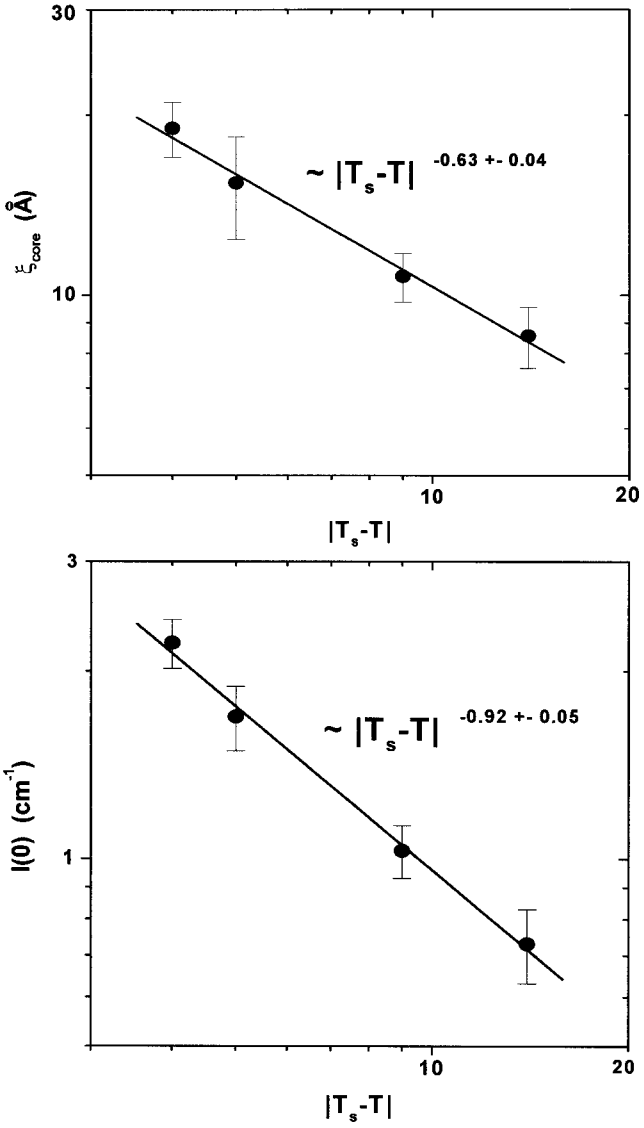

FIG. 8. Scaling of the core correlation length and $I(0)$ with $|T_s - T|$.

by Shibayama for NIPAM macrogels [36]. These facts then support the experimental findings of Li and Tanaka [7] with respect to the universality class of NIPAM gels.

ACKNOWLEDGMENTS

The authors would like to thank Dr. Mathew Hearn and Professor B. Vincent (University of Bristol) for helping with the microgel synthesis. A.F.B. wishes to thank Professor R. Pelton for helpful discussion about the surface structure of the microgel particles. All the SANS experiments were performed using the D11 expectrometer at the ILL facility. This work was supported by Ministerio de Ciencia y Tecnología (Spain) under Project No. MAT2000-1550-C03-02.

[1] A. Suzuki and T. Tanaka, Nature (London) **346**, 345 (1990); F. Ilmain, T. Tanaka, and E. Kokufuta, Nature (London) **349**, 400 (1991).
[2] F. Ilmain, T. Tanaka, and E. Kokufuta, Nature (London) **349**, 400 (1991); S. Hirotsu, Phase Transitions **47**, 183 (1994).
[3] S. Hirotsu, Adv. Polym. Sci. **110**, 1 (1993).
[4] S. Hirotsu, J. Chem. Phys. **94**, 3949 (1991).
[5] S. Hirotsu, Macromolecules **23**, 903 (1990).
[6] T. Tanaka, E. Sato, Y. Hirokawa, S. Hirotsu, and J. Peetermans, Phys. Rev. Lett. **55**, 2455 (1985).
[7] Y. Li and T. Tanaka, J. Chem. Phys. **90**, 5161 (1989).
[8] S. Hirotsu, J. Chem. Phys. **88**, 427 (1987).
[9] S. Hirotsu and A. Kaneki, in *Dynamics of Ordering Processes in Condensed Matter*, edited by S. Komura and H. Furukawa (Plenum, New York, 1987).
[10] K. K. Lee, E. L. Cusser, M. Marchetti, and M. A. McHugh, Chem. Eng. Sci. **45**, 766 (1990).
[11] J. Bastide, in *Physical Properties of Gels*, edited by J. P. Cotton-Addad (Wiley, New York, 1996).
[12] B. R. Saunders and B. Vincent, J. Chem. Soc., Faraday Trans. **92**, 3385 (1996).
[13] A. Fernández-Nieves, A. Fernández-Barbero, B. Vincent, and F. J. De las Nieves, Macromolecules **33**, 2114 (2000).
[14] A. Fernández-Nieves, A. Fernández-Barbero, and F. J. De las Nieves, J. Chem. Phys. **115**, 1 (2001).
[15] A. Fernández-Nieves, A. Fernández-Barbero, and F. J. De las Nieves (unpublished).
[16] A. Fernández-Barbero and B. Vincent, Phys. Rev. E **63**, 011509 (2000).
[17] A. Fernández-Nieves, J. V. Duijneveldt, A. Fernández-Barbero, B. Vincent, and F. J. De las Nieves, Phys. Rev. E **64**, 051603 (2001).
[18] A. Fernández-Nieves, A. Fernández-Barbero, F. J. De las Nieves, and B. Vincent, J. Phys.: Condens. Matter **12**, 3605 (2000).
[19] A. Fernández-Nieves, A. Fernández-Barbero, B. Vincent, and F. J. De las Nieves, Langmuir **17**, 1841 (2001).
[20] R. Pelton, Adv. Colloid Interface Sci. **85**, 1 (2000).
[21] X. Wu, R. H. Pelton, A. E. Hamielec, D. R. Woods, and W. McPhee, Colloid Polym. Sci. **272**, 467 (1994).
[22] S. Hirotsu, Phase Transitions **47**, 183 (1994).
[23] S. Hirotsu, Y. Hirokawa, and T. Tanaka, J. Chem. Phys. **87**, 1329 (1987).
[24] P. J. Flory, *Principles of Polymer Chemistry* (Cornell University Press, Ithaca, NY, 1953), Chaps. 12, 13.
[25] J. S. Higgins and H. C. Benoît, *Polymer and Neutron Scattering* (Oxford University Press, New York, 1996).
[26] J. Bastide and S. J. Candau, in *Physical Properties of Polymeric Gels*, edited by J. P. Cohen Addad (Wiley, Chichester, 1996).
[27] F. Brochard and P. G. de Gennes, Macromolecules **10**, 1157 (1977).
[28] P. G. De Gennes, *Scaling Concepts in Polymer Physics* (Cornell University Press, Ithaca, NY, 1979), Chap. III.
[29] A. M. Hecht, R. Duplessix, and E. Geissler, Macromolecules **18**, 2167 (1985).
[30] F. Horkay, A. M. Hecht, S. Mallam, E. Geissler, and A. R. Renie, Macromolecules **24**, 2896 (1991).
[31] S. Mallam, F. Horkay, A. M. Hecht, A. R. Renie, and E. Geissler, Macromolecules **24**, 543 (1991).
[32] H. M. Crowther, B. Saunders, S. J. Mears, T. Cosgrove, B. Vincent, S. M. Kinkg, and G.-e. Yu, Colloids Surf., A **152**, 327 (1999).
[33] For more information about the synthesis, see, for example, Ref. [20]. See also M. J. Murray and M. J. Snowden, Adv. Colloid Interface Sci. **54**, 73 (1995).
[34] See www.ill.fr
[35] B. R. Saunders, H. M. Crowther, and B. Vincent, Macromolecules **30**, 482 (1997).
[36] M. Shibayama, T. Tanaka, and C. C. Han, J. Chem. Phys. **97**, 6829 (1992).
[37] B. E. Eichinder and P. J. Flory, Trans. Faraday Soc. **64**, 2275 (1968).
[38] B. R. Saunders and B. Vincent, Colloid Polym. Sci. **275**, 9 (1997).
[39] A. Fernández-Barbero (unpublished).
[40] M. Shibayama, K. Kawakobo, and T. Norisuye, **31**, 1608 (1998).
[41] K. Kubota, S. Fujishige, and I. Ando, Polym. J. (Tokyo) **22**, 15 (1990).
[42] B. Erman and P. J. Flory, Macromolecules **19**, 2342 (1996).
[43] S. Hirotsu, J. Chem. Phys. **94**, 3949 (1991).
[44] H. Hocker, H. Shih, and P. J. Flory, Trans. Faraday Soc. **67**, 2275 (1971).
[45] K. Kratz, T. Hellweg, and W. Eimer, Polymer **42**, 6631 (2001).
[46] P. Wong, Phys. Rev. B **32**, 7417 (1985).
[47] C. Bagnuls and C. Beruillier, Phys. Rev. B **32**, 7209 (1985).
[48] C. Bagnuls and C. Beruillier, Phys. Lett. **107A**, 299 (1985).